AJNR

This information is current as of June 13, 2025.

Candidate Biomarkers of Extravascular Extracellular Space: A Direct Comparison of Apparent Diffusion Coefficient and Dynamic Contrast-Enhanced MR Imaging––Derived Measurement of the Volume of the Extravascular Extracellular Space in Glioblastoma Multiforme

S.J. Mills, C. Soh, C.J. Rose, S. Cheung, S. Zhao, G.J.M. Parker and A. Jackson

ORIGINAL RESEARCH

S.J. Mills
C. Soh
C.J. Rose
S. Cheung
S. Zhao
G.J.M. Parker
A. Jackson

Candidate Biomarkers of Extravascular Extracellular Space: A Direct Comparison of Apparent Diffusion Coefficient and Dynamic Contrast-Enhanced MR Imaging−Derived Measurement of the Volume of the Extravascular Extracellular Space in Glioblastoma Multiforme

BACKGROUND AND PURPOSE: ADC measurements have been shown to have an inverse relationship with tumor cell density. DCE-MR imaging modeling techniques can produce a measurement of the v_e, which would also be expected to have an inverse relationship with cell density. The objective of this study was to test the hypothesis that areas of increased cellularity, and therefore low ADC, would be expected to have a small EES (low v_e).

MATERIALS AND METHODS: Nineteen patients with GBM were recruited. All imaging was performed before surgery on a 3T MR imaging scanner. Imaging included diffusion tensor imaging, T1-weighted DCE-MR imaging, and anatomic sequences. Tumor VOIs were defined on the anatomic images and modified to contain only enhancing voxels. Parametric maps of ADC and v_e were generated. Statistical analysis of ADC and v_e was performed on both a voxel-by-voxel basis and comparison of median values.

RESULTS: No correlation was demonstrated between ADC and v_e in either a voxel-by-voxel analysis or comparison of median values ($P = .124$).

CONCLUSIONS: This study failed to demonstrate a correlation between ADC and v_e. This is important because it suggests that though the mechanisms underlying these parameters are theoretically similar, they actually reflect different aspects of tumor microenvironment. Consequently ADC and v_e should be considered to provide independent information about the properties of the EES.

ABBREVIATIONS: ADC = apparent diffusion coefficient; DCE-MR = dynamic contrast-enhanced MR; DWI = diffusion-weighted imaging; EES = extravascular extracellular space; FFE = fast-field echo; FLIRT = FMRIB Linear Image Registration Tool; FSL = FMRIB Software Library; FMRIB = Functional Magnetic Resonance Imaging of the Brain; GBM = glioblastoma multiforme; IAUC = initial area under the concentration curve; max = maximum; min = minimum; NSF = nephrogenic systemic fibrosis; v_e = volume of the extravascular extracellular space per unit volume; VOI = volume of interest

GBM is the most common and most aggressive primary brain tumor of adulthood. These tumors are highly heterogeneous and characterized by varying degrees of hypercellularity, cytoplasmic and nuclear pleomorphism, mitoses, and endothelial proliferation within any given tumor. A number of MR imaging−based techniques have been developed to probe the tumor microenvironment. DWI allows quantification of the degree of motion of free water molecules, resulting from Brownian motion.

ADC maps, which represent the freedom of water molecules to diffuse within tissue, can be generated. Although it has recently been demonstrated that it is possible to obtain estimates of cell packing and cell diameter in vivo,[1] the values of ADC measured by using practical clinical data acquisitions are influenced by a number of factors. ADC is affected not only by the volume of the EES but also by its spatial configuration, intracellular diffusion coefficients, and membrane permeability. However, it has been proposed that ADC is predominantly affected by extracellular geometry.[2] Thus water molecules will diffuse less freely in tissue characterized by narrow complex extracellular spaces, which might be seen in a tumor with large numbers of small cells, such as lymphoma, rather than in tissue with a smaller number of large cells in which the EES is less tortuous and in tissue in which the size of the EES is greater.

Pharmacokinetic modeling analysis of DCE-MR imaging data allows estimation of a number of parameters that affect the delivery and local distribution of the contrast molecules.

One of these is a direct estimate of the leakage volume available for contrast distribution outside the vascular space. This value (v_e) is therefore a direct estimate of the volume of the EES.[3]

Both of these techniques have been applied extensively in glioma. Changes in ADC have been demonstrated early after radiation therapy and predict treatment response (following administration of corticosteroids).[4-7] These changes are thought to reflect alterations in cellular structure due to apoptosis and/or necrosis.[4,5] A number of investigators have shown an inverse linear relationship between ADC and cell density in cerebral tumors.[5,8-10] In addition, several studies have noted an inverse relationship with malignancy and ADC, with increasing histologic tumor grade associated with low ADC values,[8,9,11,12] including high-grade tumors that were indistinguishable from low-grade tumors on conventional imaging.[13] Most DCE-MR imaging studies in glioma have evaluated vascular parameters such as blood volume and permeability, while v_e has generally been overlooked. The few studies that have examined v_e have shown it to be of value in distinguishing intra- from extra-axial tumors[14,15] and have shown it to exhibit a tendency to increase with increasing tumor grade.[14,16] In addition, v_e demonstrated sensitivity in identifying changes in response to treatment with corticosteroids, with decreases in v_e occurring following treatment, presumably reflecting a reduction in edema.[17,18]

A number of groups have performed both DCE-MR imaging and diffusion imaging in gliomas.[14,18,19] However, to the authors' knowledge, no direct comparison of ADC and v_e has been made in this tumor group. The objective of this study was to test the hypothesis that areas of increased cellularity, and therefore low ADC, would be expected to have low v_e.

Materials and Methods

Patients

The local research ethics committee approved the study, and all patients gave informed consent before recruitment. Patients with potential GBMs were identified via the neuro-oncology multidisciplinary team meetings at Salford Royal National Health Service Foundation Trust. Patients younger than 18 years of age, those unfit for surgery, and individuals in whom MR imaging was contraindicated were excluded from the outset. All imaging was performed before surgery. All tumors were histologically confirmed as GBM by either surgical debulking or biopsy, and patients in whom GBM could not be histologically confirmed postoperatively were excluded. Corticosteroids have previously been shown to alter the measurement of DCE-MR imaging parameters.[6] Withholding corticosteroid treatment was deemed unethical; therefore, all patients received corticosteroid treatment for a minimum of 48 hours before imaging as part of their standard clinical treatment and to standardize treatment across all subjects. None received any other form of treatment at the time of imaging.

Data Acquisition

Imaging was performed at the University of Manchester Magnetic Resonance Imaging Facility (Hope Hospital, Salford, United Kingdom) by using a sensitivity encoding head coil on a 3T Achieva system (Philips Medical Systems, Best, the Netherlands). Conventional anatomic sequences were chosen according to those used in routine clinical practice and included the following: axial T1-weighted inversion recovery (TR, 8.4 ms; TE, 3.8 ms; TI, 1150 ms; section thickness, 1.8 mm; 256 × 256; FOV, 240 × 240 × 324 mm), axial T2-weighted (TR, 3000 ms; TE, 80 ms; section thickness, 3.0 mm; 1024 × 1024; FOV, 266 × 266 × 135 mm), coronal T2-weighted fluid-attenuated inversion recovery (TR, 11 000 ms; TE, 120 ms; TI, 2800 ms; section thickness, 3.0 mm; 512 × 512; FOV, 230 × 230 × 195 mm), and postcontrast T1-weighted 3D volume acquisitions (TR, 9.8 ms; TE, 4. 6 ms; section thickness, 1 mm; 256 × 256; FOV, 240 × 240 × 160 mm). A 6-direction axial diffusion tensor imaging sequence (TR, 2319 ms; TE, 68 ms; section thickness, 4 mm; 128 × 128; FOV, 230 × 230 × 100 mm; b-values 0 and 1000 s/mm²; Δ, 33.5 ms) was acquired.

For the DCE-MR imaging acquisitions, the orientation was altered to a sagittal-oblique plane to incorporate the internal carotid artery for measurement of an arterial input function. Four precontrast T1-FFE (radio-frequency-spoiled gradient echo) sequences (2°, 5°, 10°, 16°) were acquired in the same geometry for calculation of baseline T1 maps (TR, 3.5 ms; TE, 1.1 ms; section thickness, 4.2 mm; 128 × 128; FOV, 230 × 230 × 105 mm) with the standard variable flip angle method for T1 estimation being used.[20] This was followed by a dynamic contrast-enhanced acquisition series (TR, 3.5 ms; TE, 1.1 ms; flip angle, 16°; section thickness, 4.2 mm; 128 × 128; FOV, 230 × 230 × 105 mm) consisting of 100 volumes with temporal spacing of approximately 3.4 seconds. Gadolinium-based contrast agent (gadopentetate dimeglumine bis-methylamide, Omniscan; GE Healthcare, Oslo, Norway) was injected as a bolus dose of 0.1-mmol/kg⁻¹ of body weight, at a rate of 3 mLs⁻¹, after acquisition of the fifth image volume. Pre- and postcontrast T1-weighted imaging sequences (TR, 9.3 ms; TE, 4.6 ms) were acquired in the same sagittal oblique geometry for definition of VOI of the whole tumor.

Data Processing

VOIs were defined for each tumor by an experienced radiologist (S.J.M.), before histologic diagnosis was confirmed. Analysis was performed by using in-house software (Manchester Dynamic Modeling) and the extended Tofts and Kermode pharmacokinetic model.[21] Automated arterial input functions were generated from an appropriately chosen section that included the internal carotid artery.[22] Parametric maps of the IAUC were produced. ADC maps were generated by using DTIStudio (Johns Hopkins University, Baltimore, Maryland).[23]

Tumor VOIs were modified to contain only voxels with contrast—that is with an initial IAUC during the first 60 seconds (IAUC$_{60}$) >0 mmol/s. Parametric maps of ADC and v_e were generated. Axial ADC and sagittal oblique v_e images were coregistered by using the FLIRT linear registration in the FSL package.[24] The $b = 0$ image was used as the reference image, and the 2° T1-FFE was used as the input image. An affine 12-parameter registration with a normalized correlation (intramodal) cost function and nearest neighbor interpolation was applied. The derived transformation was then applied to the sagittal oblique v_e parametric map. This generated an axially oriented v_e map, which could be overlaid on the ADC for voxel-by-voxel analysis (Fig 1).

Statistical Analysis

Scatterplots of ADC and v_e were generated for both a voxel-by-voxel analysis and comparison of median values. In addition, a scatterplot of ADC versus v_e, with low values of v_e (<0.05) excluded, was generated. This was an attempt to overcome potential v_e modeling problems, in which very low values of v_e may be the result of underperfused
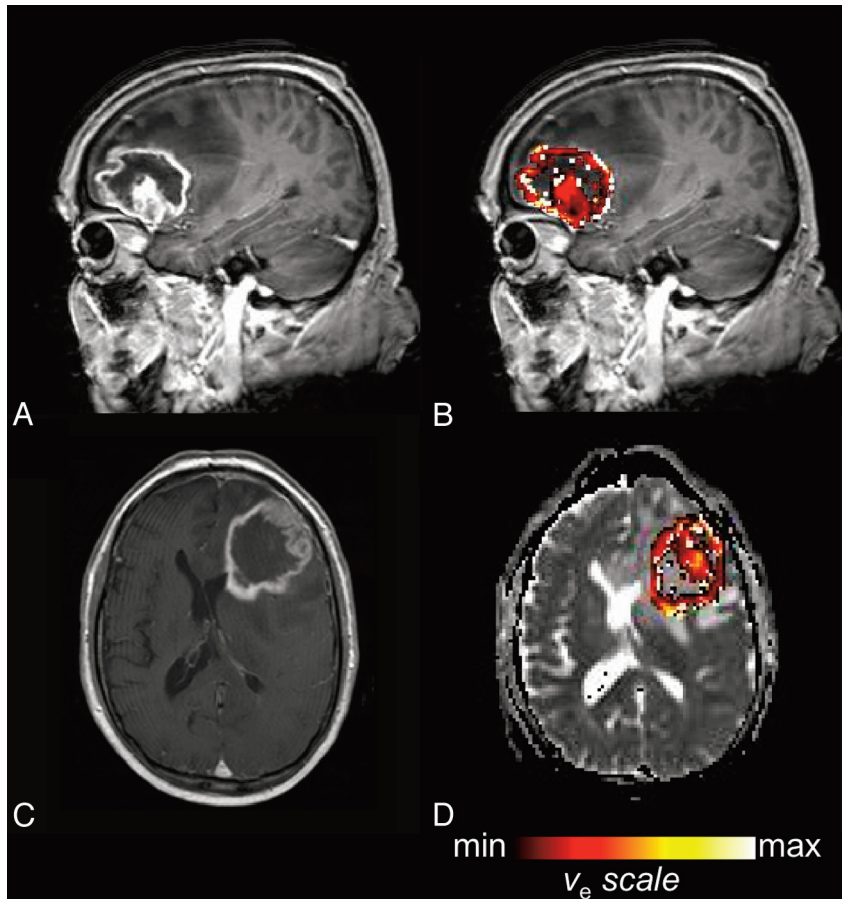
Fig 1. *A* and *B*, Sagittal oblique postcontrast T1-weighted image (*A*) depicting a left frontal GBM with v_e (unitless) map overlaid (*B*). *C*, Axial postcontrast T1-weighted image. *D*, Axial ADC map with coregistered v_e map overlaid and v_e color scale bar.

tissue in which there is no leakage of contrast into the EES. Where appropriate, SPSS version 15.0 (SPSS, Chicago, Illinois) was used for bivariate Spearman correlation analysis to identify a relationship between the 2 parameters.

Results

Patients
Nineteen patients (7 men, 11 women; age range, 18–77 years; mean age, 60 ± 12 years) with histologically confirmed GBM were included in the study. An additional 2 patients were excluded due to lack of histologic confirmation of GBM.

Voxel-by-Voxel Analysis
Figure 2 shows a typical sample scatterplot from 1 individual illustrating the voxel-by-voxel comparison of ADC and v_e. These plots show no evidence of a linear relationship between ADC and v_e in any case. Removal of very low values of v_e (< 0.05) also showed no linear relationship between the 2 parameters (Fig 3).

Comparison of Median Values
Figure 4 demonstrates the scatterplot of median values of ADC versus median values of v_e. A Spearman bivariate correlation analysis showed no significant relationship between the 2 parameters (*P* = .124).
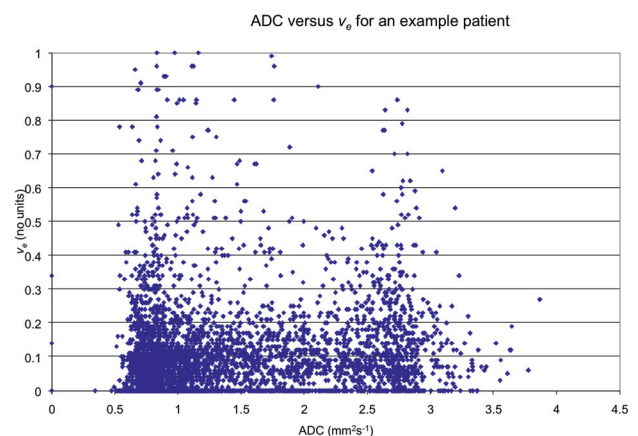

Fig 2. Scatterplot of a voxel-by-voxel comparison of ADC and v_e (no units) for 1 sample patient. No relationship is demonstrated between the 2 parameters.

Discussion

There is a pressing requirement for imaging biomarkers that can provide information reflecting tumor cell numbers, cell size, and cell packing. In oncologic practice, there is an increasing need to monitor the effects of tumor phenotypes and novel therapeutics on cellular proliferation and cell death. Mapping the size and spatial characteristics of the EES is one of the most promising approaches, and a number of groups have already described relationships between diffusion and enhancement characteristics and cellular structure.[14,15] Several
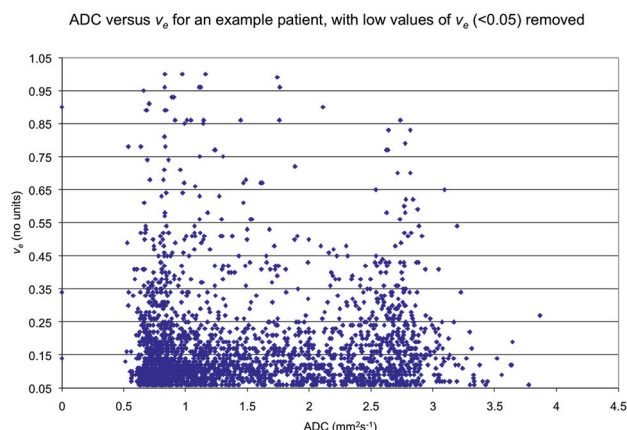
ADC versus v_e for an example patient, with low values of v_e (<0.05) removed

Fig 3. Scatterplot of a voxel-by-voxel comparison of ADC and v_e (no units) with low values of v_e removed for 1 sample patient. Low values of v_e may under-represent the EES because they may occur as a result of underperfusion and minimal contrast leakage into the EES. No relationship is demonstrated between the 2 parameters.
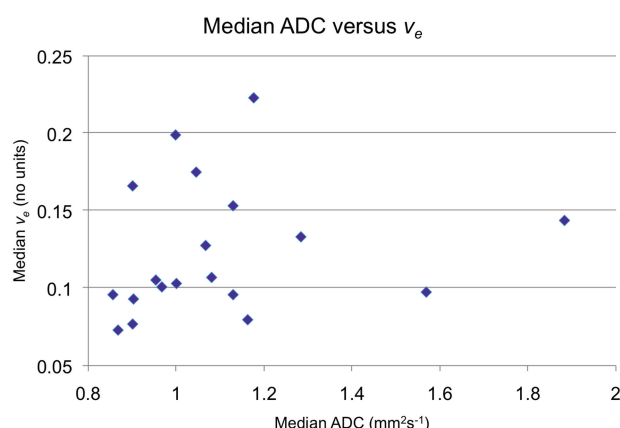

Median ADC versus v_e

Fig 4. Scatterplot of a comparison of the median values of ADC versus v_e (no units).

groups have reported an inverse correlation of ADC with cell density in gliomas,[5,8-10] and the measurement v_e from DCE-MR imaging is thought to reflect EES volume. Indeed, similar changes were reported in both parameters following treatment with glucocorticoid steroids, with reductions in both ADC and v_e.[18] Both techniques, therefore, present us with promising candidate biomarkers for the study of cellular structure. In theory, these parameters are both heavily influenced by the volume of the EES, and we, therefore, hypothesized that these 2 measures should correlate. However, we were unable to identify any evidence of such a relationship on either a voxel-by-voxel basis or by comparison of median values.

The negative results of this study are important because they indicate that our current conceptual understanding of these parameters is incomplete. This indicates the need for further evaluation of the features in the tumor microenvironment that affect each set of parameters if we are to use them as the basis for useful biomarkers of cellular structure.

While no study has directly compared v_e and ADC in glioma, a study of therapeutic response in breast carcinoma by Yankeelov et al[25] reported a negative correlation between these 2 parameters, with ADC increasing and v_e decreasing following treatment. They hypothesized that these findings

may reflect a decrease in interstitial fluid pressure following treatment, aiding the elimination of cell debris and causing an increase in ADC but an overall decrease in v_e.[25] They also acknowledged the difficulties in measuring ADC accurately in breast tissue and how their findings differ from the those in the literature, in which studies of ADC values alone have reported decreases following treatment for breast cancer,[26-31] which is in keeping with the changes in ADC values seen in glioma following treatment.[4-7]

There are potential methodologic problems with this study in the measurement of both parameters. A number of factors can influence measurements derived from DWI. The calculation of ADC is based on the difference in observed signal intensity, which occurs as a result of diffusion between temporally separated dephasing and rephasing gradients. The magnitude, duration, and temporal separation of these matched gradients will each have a separate effect on the magnitude of the resulting signal-intensity drop observed. Thus calculated ADC values will be affected not only by the volume of the EES but also by the complexity and absolute dimensions of the EES. Diffusion signal intensity can also be affected by capillary bed perfusion, intracellular diffusion coefficients, membrane permeability, and exchange times.[32]

The heterogeneous nature of GBMs with areas of microvascular proliferation, necrosis, cyst formation, edema, and increased cellularity will, therefore, have the potential to influence the ADC values in a number of different ways. Areas of microvascular proliferation and increased perfusion may influence the diffusion signal intensity, though a relatively high b-value of 1000 s/mm^{-2} was used in this study, so capillary perfusion should not have significantly contributed to the signal intensity.[32,33] Necrotic cells, debris, and hemorrhage also can restrict movement of water in the EES and decrease measured ADC values. Cystic areas are reflected by high ADC values,[34] while areas of increased cellularity are associated with low ADC values.[5,8-10] Destruction of the blood-brain barrier and alterations in cell permeability will also affect the intra- and extracellular diffusion coefficients and exchange times, again influencing the ADC values.

The heterogeneity of GBMs complicates analysis further. While attempts were made to overcome the problems of regional heterogeneity by performing a voxel-by-voxel analysis of the data and excluding voxels that contained no contrast (and therefore were likely to represent solely cystic or necrotic material), no correction could be made for heterogeneity beyond the resolution of the voxel. Recently, a study by Sadeghi et al[35] found an inverse relationship between ADC values and microvessel density in bulk tumor, which was not present in peritumoral or infiltrated tissue. They hypothesized that the ADC values within the bulk tumor and peritumoral tissue were influenced by different factors, with edema and components of the extracellular matrix having a more predominant effect on ADC values in the peritumoral tissue than either cell or vessel density. Unlike a number of previous studies,[5,8-10] Sadeghi's group failed to find a significant relationship between ADC values and cell density.

There are also potential modeling problems associated with the calculation of v_e. By definition, v_e can only be measured when contrast medium leaks from the vessels into the EES. Thus v_e cannot be estimated in tissue that is unperfused

or when no extravascular contrast leakage occurs. This means that there may be a significant number of voxels within each tumor that show very low/unmeasureable v_e and a wide range of possible ADC values. Figure 2 provides some evidence that this may indeed be the case. However, if the low values of v_e are removed from Fig 2, there is still no clear relationship between v_e and ADC (Fig 3).

One final limitation of the study is the use of Omniscan contrast agent, which has decreased dramatically as a result of its association with NSF.[36] Agents that have a lower reported risk of NSF, such as gadolinium diethylene triamine pentaacetic acid (Magnevist; Bayer Schering Pharma, Berlin, Germany) and gadoterate meglunine (Dotarem; Guerbet, Paris, France), have T1 relaxivity properties similar to those of Omniscan (4.3 and 4.2 L/mmol/s respectively versus 4.6 L/mmol/s)[37,38] and are, therefore, unlikely to have significant effects on the v_e measurements if the study was repeated with an alternative contrast agent.

Conclusions

Although ADC and v_e are believed to reflect the size of the EES, these measurements did not correlate in patients with GBM. These results suggest that the current interpretation of these parameters is oversimplistic and that they provide independent information about the tumor microenvironment. The lack of correlation may result from methodologic variations in either or both measurements. This study highlights the requirement for further development and evaluation of proposed biomarkers that describe aspects of the tumor microstructure.

References

1. Alexander DC, Hubbard PL, Hall MG, et al. **Orientationally invariant axon-size and density weighted MRI.** *In: Proceedings of the International Society for Magnetic Resonance in Medicine,* Honolulu, Hawaii. April 18-24, 2009
2. Sen PN, Basser PJ. **A model for diffusion in white matter in the brain.** *Biophys J* 2005;89:2927–38
3. Tofts PS, Brix G, Buckley DL, et al. **Estimating kinetic parameters from dynamic contrast-enhanced T1-weighted MRI of a diffusable tracer: standardized quantities and symbols.** *J Magn Reson Imaging* 1999;10:223–32
4. Moffat BA, Chenevert TL, Lawrence TS, et al. **Functional diffusion map: a noninvasive MRI biomarker for early stratification of clinical brain tumor response.** *Proc Natl Acad Sci U S A* 2005;102:5524–29
5. Chenevert TL, Stegman LD, Taylor JM, et al. **Diffusion magnetic resonance imaging: an early surrogate marker of therapeutic efficacy in brain tumors.** *J Natl Cancer Inst* 2000;92:2029–36
6. Bastin ME, Carpenter TK, Armitage PA, et al. **Effects of dexamethasone on cerebral perfusion and water diffusion in patients with high-grade glioma.** *AJNR Am J Neuroradiol* 2006;27:402–08
7. Bastin ME, Delgado M, Whittle IR, et al. **The use of diffusion tensor imaging in quantifying the effect of dexamethasone on brain tumours.** *Neuroreport* 1999;10:1385–91
8. Sugahara T, Korogi Y, Kochi M, et al. **Usefulness of diffusion-weighted MRI with echo-planar technique in the evaluation of cellularity in gliomas.** *J Magn Reson Imaging* 1999;9:53–60
9. Kono K, Inoue Y, Nakayama K, et al. **The role of diffusion-weighted imaging in patients with brain tumors.** *AJNR Am J Neuroradiol* 2001;22:1081–88
10. Guo AC, Cummings TJ, Dash RC, et al. **Lymphomas and high-grade astrocytomas: comparison of water diffusibility and histologic characteristics.** *Radiology* 2002;224:177–83
11. Yang D, Korogi Y, Sugahara T, et al. **Cerebral gliomas: prospective comparison of multivoxel 2D chemical-shift imaging proton MR spectroscopy, echoplanar perfusion and diffusion-weighted MRI.** *Neuroradiology* 2002;44:656–66
12. Yamasaki F, Kurisu K, Satoh K, et al. **Apparent diffusion coefficient of human brain tumors at MR imaging.** *Radiology* 2005;235:985–91
13. Lee EJ, Lee SK, Agid R, et al. **Preoperative grading of presumptive low-grade astrocytomas on MR imaging: diagnostic value of minimum apparent diffusion coefficient.** *AJNR Am J Neuroradiol* 2008;29:1872–77
14. Ludemann L, Grieger W, Wurm R, et al. **Quantitative measurement of leakage volume and permeability in gliomas, meningiomas and brain metastases with dynamic contrast-enhanced MRI.** *Magn Reson Imaging* 2005;23:833–41
15. Zhu XP, Li KL, Kamaly-Asl ID, et al. **Quantification of endothelial permeability, leakage space, and blood volume in brain tumors using combined T1 and T2* contrast-enhanced dynamic MR imaging.** *J Magn Reson Imaging* 2000;11:575–85
16. Ludemann L, Grieger W, Wurm R, et al. **Comparison of dynamic contrast-enhanced MRI with WHO tumor grading for gliomas.** *Eur Radiol* 2001;11:1231–41
17. Andersen C, Jensen FT. **Differences in blood-tumour-barrier leakage of human intracranial tumours: quantitative monitoring of vasogenic oedema and its response to glucocorticoid treatment.** *Acta Neurochir (Wien)* 1998;140:919–24
18. Armitage PA, Schwindack C, Bastin ME, et al. **Quantitative assessment of intracranial tumor response to dexamethasone using diffusion, perfusion and permeability magnetic resonance imaging.** *Magn Reson Imaging* 2007;25:303–10
19. McMillan KM, Rogers BP, Koay CG, et al. **An objective method for combining multi-parametric MRI datasets to characterize malignant tumors.** *Med Phys* 2007;34:1053–61
20. Fram EK, Herfkens RJ, Johnson GA, et al. **Rapid calculation of T1 using variable flip angle gradient refocused imaging.** *Magn Reson Imaging* 1987;5:201–08
21. Tofts PS. **Modeling tracer kinetics in dynamic Gd-DTPA MR imaging.** *J Magn Reson Imaging* 1997;7:91–101
22. Parker GJ, Jackson A, Waterton JC, et al. **Automated arterial input function extraction for T1-weighted DCE-MRI.** In: *Proceedings of the 11th Annual Meeting of International Society for Magnetic Resonance in Medicine,* Toronto, Ontario, Canada. July 10–16, 2003:Abstract No. 1264
23. Jiang H, van Zijl PC, Kim J, et al. **DTIStudio: resource program for diffusion tensor computation and fiber bundle tracking.** *Comput Methods Programs Biomed* 2006;81:106–16
24. Jenkinson M, Smith S. **A global optimisation method for robust affine registration of brain images.** *Med Image Anal* 2001;5:143–56
25. Yankeelov TE, Lepage M, Chakravarthy A, et al. **Integration of quantitative DCE-MRI and ADC mapping to monitor treatment response in human breast cancer: initial results.** *Magn Reson Imaging* 2007;25:1–13
26. Guo Y, Cai YQ, Cai ZL, et al. **Differentiation of clinically benign and malignant breast lesions using diffusion-weighted imaging.** *J Magn Reson Imaging* 2002;16:172–78
27. Kinoshita T, Yashiro N, Ihara N, et al. **Diffusion-weighted half-Fourier single-shot turbo spin echo imaging in breast tumors: differentiation of invasive ductal carcinoma from fibroadenoma.** *J Comput Assist Tomogr* 2002;26:1042–46
28. Kuroki Y, Nasu K, Kuroki S, et al. **Diffusion-weighted imaging of breast cancer with the sensitivity encoding technique: analysis of the apparent diffusion coefficient value.** *Magn Reson Med Sci* 2004;3:79–85
29. Sinha S, Lucas-Quesada FA, Sinha U, et al. **In vivo diffusion-weighted MRI of the breast: potential for lesion characterization.** *J Magn Reson Imaging* 2002;15:693–704
30. Woodhams R, Matsunaga K, Iwabuchi K, et al. **Diffusion-weighted imaging of malignant breast tumors: the usefulness of apparent diffusion coefficient (ADC) value and ADC map for the detection of malignant breast tumors and evaluation of cancer extension.** *J Comput Assist Tomogr* 2005;29:644–49
31. Woodhams R, Matsunaga K, Kan S, et al. **ADC mapping of benign and malignant breast tumors.** *Magn Reson Med Sci* 2005;4:35–42
32. Norris DG. **The effects of microscopic tissue parameters on the diffusion weighted magnetic resonance imaging experiment.** *NMR Biomed* 2001;14:77–93
33. Le Bihan D, Breton E, Lallemand D, et al. **MR imaging of intravoxel incoherent motions: application to diffusion and perfusion in neurologic disorders.** *Radiology* 1986;161:401–07
34. Brunberg JA, Chenevert TL, McKeever PE, et al. **In vivo MR determination of water diffusion coefficients and diffusion anisotropy: correlation with structural alteration in gliomas of the cerebral hemispheres.** *AJNR Am J Neuroradiol* 1995;16:361–71
35. Sadeghi N, D'Haene N, Decaestecker C, et al. **Apparent diffusion coefficient and cerebral blood volume in brain gliomas: relation to tumor cell density and tumor microvessel density based on stereotactic biopsies.** *AJNR Am J Neuroradiol* 2008;29:476–82
36. Shellock FG, Spinazzi A. **MRI safety update 2008. Part 1. MRI contrast agents and nephrogenic systemic fibrosis.** *AJR Am J Roentgenol* 2008;191:1129–39
37. Bellin MF, Van Der Molen AJ. **Extracellular gadolinium-based contrast media: an overview.** *Eur J Radiol* 2008;66:160–67
38. van der Molen AJ, Bellin MF. **Extracellular gadolinium-based contrast media: differences in diagnostic efficacy.** *Eur J Radiol* 2008;66:168–74